

Saturation of spin-polarized current in nanometer scale aluminum grains

Y. G. Wei, C. E. Malec, and D. Davidović

School of Physics, Georgia Institute of Technology, Atlanta, Georgia 30332, USA

(Received 15 October 2007; published 27 November 2007)

We describe measurements of spin-polarized tunneling via discrete energy levels of single aluminum grains. In high resistance samples ($\sim G\Omega$), the spin-polarized tunneling current rapidly saturates as a function of the bias voltage. This indicates that the spin-polarized current is carried only via the ground state and the few lowest in energy excited states of this grain. At the saturation voltage, the spin-relaxation rate T_1^{-1} of the highest states excited by tunneling is comparable to the electron tunneling rate, $T_1^{-1} \approx 1.5 \times 10^6$ and 10^7 s $^{-1}$, in two samples. The ratio of T_1^{-1} to the electron-phonon relaxation rate is in agreement with the Elliot-Yafet scaling, an evidence that spin relaxation in Al grains is governed by the spin-orbit interaction.

DOI: [10.1103/PhysRevB.76.195327](https://doi.org/10.1103/PhysRevB.76.195327)

PACS number(s): 73.21.La, 72.25.Hg, 72.25.Rb, 73.23.Hk

I. INTRODUCTION

Electron tunneling through single nanometer scale metallic grains at low temperatures can display a discrete energy level spectrum.¹ Tunneling spectroscopy of the energy spectra has led to numerous discoveries, including Fermi-liquid coupling constants between quasiparticles,² spin-orbit interactions,^{3,4} and superconducting correlations in zero-dimensional systems.⁵ Some information regarding the spin of an electron occupying a discrete level can be obtained using spin-unpolarized tunneling, such as spin-multiplicity and electron g factors.¹

In this paper, we report on spin-polarized tunneling via discrete energy levels of single aluminum grains. Spin-polarized electron transport permits studies of spin relaxation and spin dephasing.^{6,7} By comparison, spin-unpolarized spectroscopy is suitable for the studies of energy relaxation in the grains.^{1,2} Since spin-relaxation times are generally many orders of magnitude longer than energy relaxation times, spin-unpolarized spectroscopy is not an easy tool to study spin relaxation in the grains, and spin-polarized tunneling is needed. We find that some electron spin-relaxation times in Al grains are exceptionally long compared to bulk Al with similar disorder, on the order of microseconds.

Spin-polarized transport via metallic grains has recently generated a lot of theoretical interest.⁸⁻¹² In addition, there is a major effort to study nanospintronics using carbon nanotubes; see Ref. 13 and references therein. Spin-coherent electron tunneling via nanometer scale normal metallic grains has been confirmed in arrays^{14,15} and in single grains.¹⁶ However, the electron spin-relaxation time T_1 in a metallic grain has not been reported yet.

II. SAMPLE FABRICATION

Our samples are prepared by electron beam lithography and shadow evaporation, similar to the technique described previously.³ First, we define a resist bridge placed 250 nm above the Si wafer; this bridge acts as a mask. Next [Fig. 1(A)], we deposit 11 nm Permalloy (Py=Ni_{0.8}Fe_{0.2}) onto oxidized silicon substrate at 4×10^{-7} Torr base pressure, measured near the gate valve, along the direction indicated by the arrow. Then, we rotate the sample by 36° with-

out breaking the vacuum and deposit 1.2 nm of Al₂O₃ by reactive evaporation of Al,³ at a rate of 0.35 nm/s and at an oxygen pressure of 2.5×10^{-5} Torr. Now, oxygen flow is shut down. When pressure decreases to the 10^{-7} Torr range, we deposit a 0.6 nm thick film of Al, as shown in Fig. 1(B). Al forms isolated grains with a typical diameter of 5 nm. The grains are displayed by the scanning electron microscope (SEM) image in Fig. 1(D). Finally, we deposit another 1.2 nm layer of Al₂O₃ by the reactive evaporation and top it of an 11 nm thick film of Py [Fig. 1(C)]. We make many samples on the same silicon wafer, and vary the overlap from 0 to 50 nm and select the devices with the highest resistance, as they have the smallest overlap. Figures 1(E) and 1(F) show SEM images of a typical device.

III. DISCRETE ENERGY LEVELS

Transport properties of the samples at low temperatures were measured using an Ithaco current amplifier. The samples were cooled down to ≈ 0.035 K base temperature. The sample leads were cryogenically filtered to reduce the electron temperature down to ≈ 0.1 K.

The majority of samples (>80%) exhibit Coulomb blockade at low temperature. About 150 samples were measured at 4.2 K and 16 samples at 0.035 K. In this paper, we describe two samples. The I - V curves of two samples are shown in Figs. 1(G) and 1(H). The tunneling current increases in discrete steps as a function of bias voltage, corresponding to discrete electron-in-a-box energy levels of the grain.

In sample 1, the average electron-in-a-box level spacing caused by electron geometric confinement is $\delta \approx 0.8$ meV, which corresponds to diameter $D \approx 6$ nm assuming a spherical Al grain. The average current step $\bar{I} \approx 0.47$ pA. We make a connection with the tunneling rates from the leads to the grain and the measured current response. The tunnel junctions are highly asymmetric, and therefore, one of the tunneling rates is much smaller than the other, and thus rate limiting. Throughout this paper, we choose the rate limiting step to be across the left junction, corresponding to the tunneling rate Γ_L . Therefore, our measured current corresponds to the average tunneling-in rate of $\bar{\Gamma}_L = \bar{I}/2|e| \approx 1.5 \times 10^6$ s $^{-1}$. Similarly, in sample 2, $\delta \approx 2.7$ meV, $D \approx 4$ nm, and $\bar{\Gamma}_L \approx 9.6 \times 10^6$ s $^{-1}$.

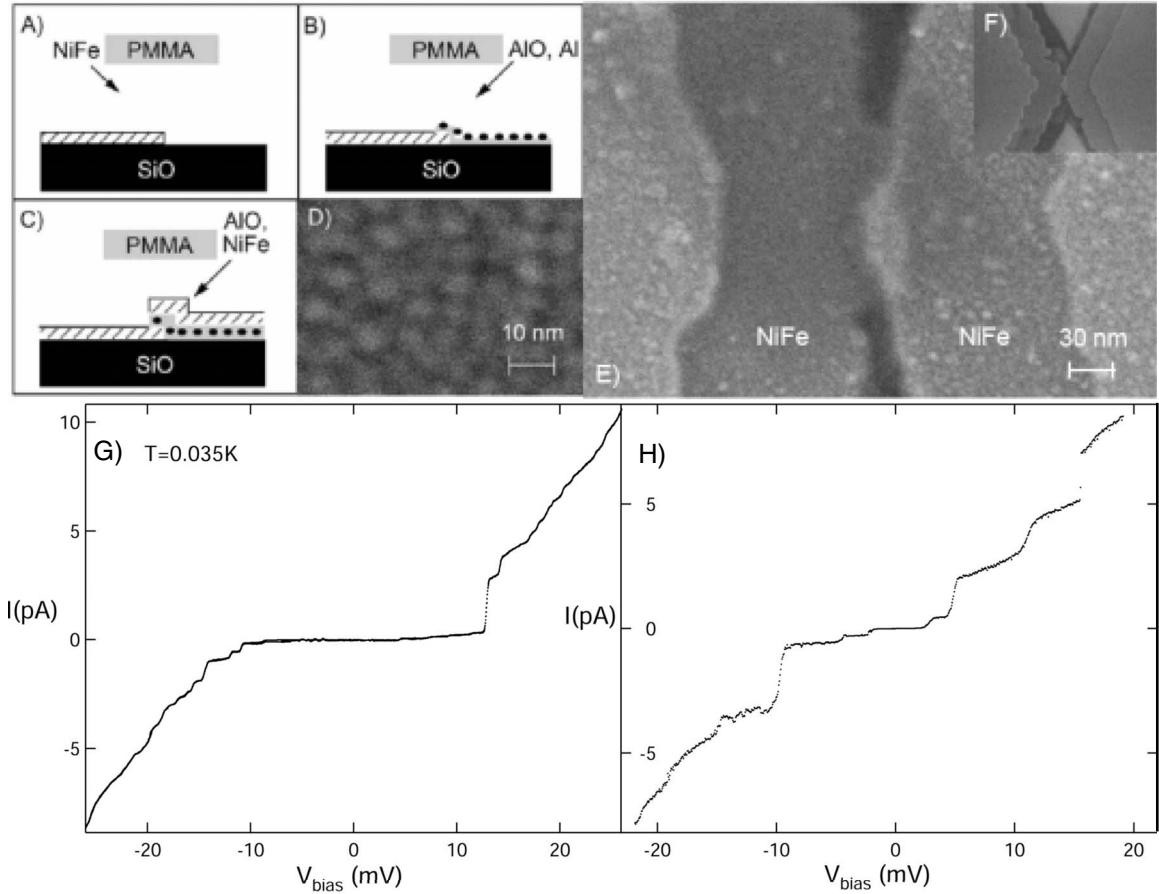


FIG. 1. (A), (B), and (C): sample fabrication steps. (D): image of Al grains. (E) and (F): image of a typical sample. (G) and (H): I - V curves at the base temperature.

The spin-conserving energy relaxation in Al grains takes place by phonon emission with the relaxation rate,²

$$\tau_{e-ph}^{-1}(\omega) = \left(\frac{2}{3}E_F\right)^2 \frac{\omega^3 \tau_e \delta}{2\rho \hbar^5 v_s^5}, \quad (1)$$

where $E_F=11.7$ eV is the Fermi energy, ω is the energy difference between the initial and the final states, $\rho=2.7$ g/cm³ is the ion-mass density, and $v_s=6420$ m/s is the sound velocity. We obtain $\tau_{e-ph}^{-1}(\delta) \approx 1.6 \times 10^9$ and 4.1×10^{10} s⁻¹ in samples 1 and 2, respectively. Sample 2 has significantly larger relaxation rate because of the larger level spacing. Since the tunneling rates in our samples are $\sim 10^6$ s⁻¹, if the grain is excited by electron tunneling in and out, it will instantly relax to the lowest energy state accessible by spin-conserving transitions.

As shown by Fig. 2, the energy levels exhibit Zeeman splitting as a function of an applied magnetic field. In sample 1, the I - V curve probes the same energy spectrum at negative and positive bias voltages. This is evident from the equivalence of the magnetic field dependencies at negative and positive biases. The lowest tunneling threshold is twofold degenerate at zero magnetic field, showing that N_0 , the number of electrons on the grain before tunneling in, is even. The conductance peaks are similar in magnitude at negative bias, because the first tunneling step, in which an electron tunnels

into the grain through the higher resistance junction, is rate limiting. At positive bias, the first conductance peak is much larger than the subsequent conductance peaks, because the first tunneling step takes place via the lower resistance junction, and the rates are limited by the electron discharge process across the high resistance junction.

In sample 1, the first two peaks corresponding to g factors: $g=1.83 \pm 0.05$ and 1.95 ± 0.05 . Slight reduction of the g factors from sample 2 indicates spin-orbit interaction in Al.¹ The avoided level crossings are clearly resolved in Fig. 2, near points $(-11.5$ mV, 5 T) and $(-13$ mV, 11.5 T). The corresponding avoided crossings at positive bias are located near $(13.5$ mV, 5 T) and $(15.5$ mV, 11.5 T), respectively. In the regime, where g factors are slightly reduced, the spin-orbit scattering rate (τ_{SO}^{-1}) can be obtained from the avoided crossing energies $\Delta_{SO} \approx 0.1$ meV.¹⁷ Theory predicts that $\tau_{SO} \approx \hbar \delta / \pi \Delta_{SO}^2$,¹⁷ within a factor of 2. Thus, we obtain $\tau_{SO}^{-1} \approx 5.5 \times 10^{10}$ s⁻¹. By the Elliot-Yafet relation,¹⁸ τ_{SO}^{-1} is related to the elastic scattering rate τ_e^{-1} : $\tau_{SO}^{-1} = \alpha \tau_e^{-1}$. Assuming ballistic grain, $\tau_e^{-1} \approx v_F / D = 3.4 \times 10^{14}$ s⁻¹. We obtain $\alpha \approx 1.6 \times 10^{-4}$, in excellent agreement with $\alpha \approx 10^{-4}$ in Al thin films.¹⁹

IV. SPIN-POLARIZED TUNNELING

Now, we discuss magnetoresistance from the spin-polarized tunneling. In the magnetic field range of ± 50 mT,

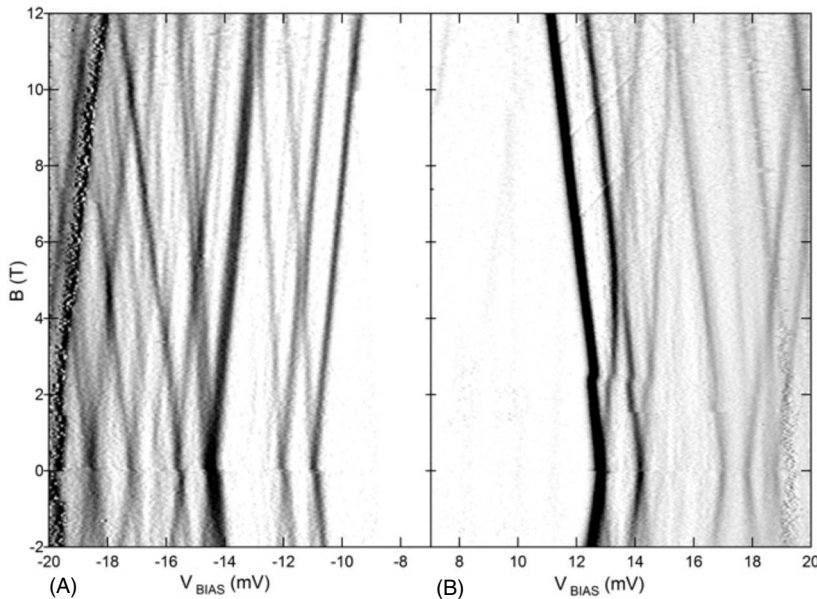


FIG. 2. (A) and (B): differential conductance peaks (dark) versus bias voltage and the applied magnetic field in sample 1 at the base temperature.

approximately 90% of the samples do not display any of the tunneling magnetoresistance (TMR) effect. By contrast, we tested about ten tunneling junctions without the embedded grains and with similar resistance (empty junctions) at 4.2 K. All of the empty junctions exhibit a significant TMR in this field range, comparable to 10%. Approximately one-half of the empty junctions display a simple spin-valve effect. So the absence of TMR for electron tunneling via grains shows that the spin-dephasing rate T_2^{-1} in 90% of the samples must be much larger than the tunneling rate.

Nevertheless, approximately 10% of the samples with embedded grains display significant TMR, so the dephasing must be weak, e.g., T_2^{-1} must be smaller than or comparable to the tunneling rate in these samples. Here, T_2 variation among different samples could be explained by magnetic defects, such as paramagnetic impurities from the Py layer. Paramagnetic impurities are common sources of dephasing.²⁰ The defects would be located on the grain surface, since bulk Al does not support paramagnetism. Since the number of atoms on the surface is relatively small (~ 1000), we could occasionally obtain a sample free of impurities. More insight into the nature of T_2 in this device will require a more in depth theoretical study.

Majority of the samples with nonzero TMR show positive TMR near the Coulomb-blockade conduction threshold; only about 30% of the samples show negative TMR. The sign of TMR in quantum dots is determined by the interplay between charging effects and spin accumulation.^{15,21} For any given sample, the data in this paper correspond to the voltage range within the first step of the Coulomb staircase. In this range, the sign of TMR is found to be constant as expected.

TMR in our devices usually does not display a simple spin-valve effect. We believe that this is because there are spin-dependent interactions inside the grain, which induce a complicated TMR even when the magnetic transitions in the drain and source leads are sharp as expected. For example, a rotation of stray magnetic field acting on the grain will alter the direction of the spin-quantization axis in the grain, thereby changing the conductance.⁸ A rotation or a switch of

a remote domain can change the tunneling current through the grain via the magnetic field generated by the domain. Similarly, the orientation of the nuclear spin in the grain can change the quantization axes via the hyperfine interaction.

We select only those samples that display a simple spin-valve TMR effect, which is shown in Figs. 3. Figure 3(A) is the TMR of sample 1 at a bias voltage corresponding to the second current plateau. TMR is barely resolved in this case, since the current changes by only about 40 fA. We do not have good data to display TMR at the first current plateau. By comparison, Figs. 3(B) and 3(C) display TMR at bias voltage where the numbers of electron-in-a-box levels energetically available for tunneling in are approximately 19 and 48, respectively. To facilitate comparisons, the current intervals on the vertical axes in Figs. 3(A)–3(C) and 3(D)–3(F) have equal lengths.

The main observation in this paper is that $\Delta I = I_{\uparrow\uparrow} - I_{\uparrow\downarrow}$ is nearly constant with current above a certain current. There is hardly any increase in ΔI between Figs. 3(B) and 3(C) and between Figs. 3(E) and 3(F). This behavior is shown in more detail in Fig. 4(A) and 4(B), which displays ΔI versus bias voltage. Here, ΔI versus negative bias voltage in sample 1 is fully saturated at the third current plateau; at the second current plateau, ΔI is already at one-half of the saturation value. Similarly, in sample 2, ΔI reaches saturation at the second current plateau. Our samples should be contrasted with ordinary ferromagnetic tunneling junctions, where ΔI is proportional to the current over a significantly wider range of bias voltage.^{22,23}

V. INTERPRETATION OF THE RESULTS

In Coulomb-blockade samples containing magnetic leads, the electrochemical potential difference between the island and leads can jump when the magnetization in one of the leads changes direction.¹⁰ This can lead to a sudden shift in energy levels, producing a jump in current that is constant as a function of bias voltage. The shift in energy levels is seen

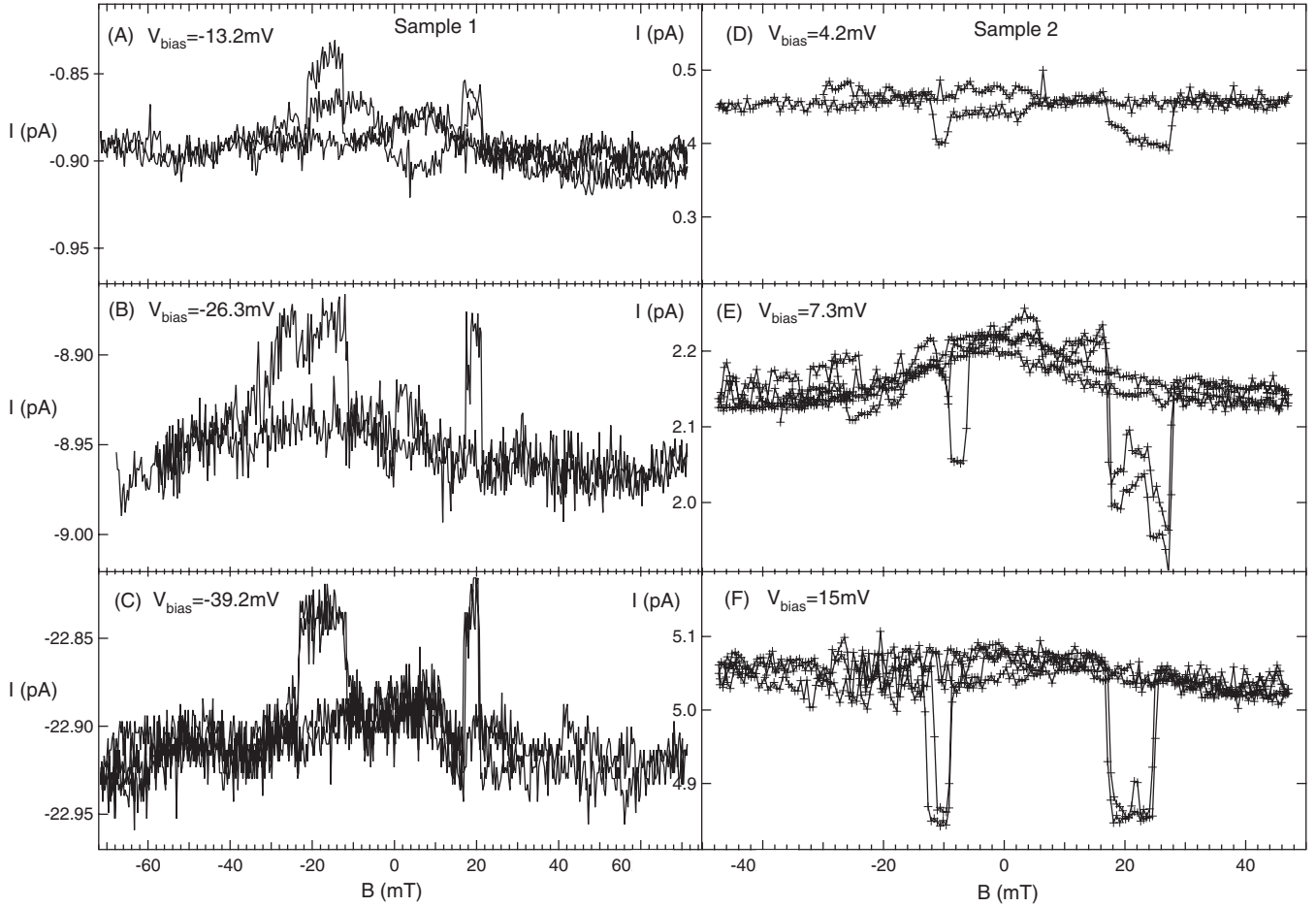


FIG. 3. (A)–(F): spin-valve effect in current versus applied magnetic field in two samples at the base temperature. The current magnitude is reduced in the antiparallel state.

as a discontinuity near zero magnetic field in Fig. 2 and is ~ 0.1 mV.

To show that the electrochemical shift is not responsible for the saturation of the spin-polarized current with voltage in our sample, we performed other measurements by sweeping the magnetic field both on and between the current plateaus, coming up with similar values for the electrochemical shift. The shift is lower than the average level spacings of 0.8 and 2.7 meV for sample 1 and sample 2, respectively. Therefore, since we measured magnetoresistance in the middle of the current plateau, the threshold voltage shift should not affect our measurements of the saturation in ΔI .

To explain $I_{\uparrow\uparrow} - I_{\uparrow\downarrow} = \text{const}$, we must discuss the relative magnitudes of three rates: τ_{e-ph}^{-1} , the rate of energy relaxation from excited to lower energy states by spin-conserving phonon emission; Γ_L , the rate electrons tunnel into the grain; and T_1^{-1} , the rate of transitions between levels that result in an electron flipping in its spin orientation. Moreover, τ_{e-ph}^{-1} is obtained theoretically, the measured I - V spectrum fixes the tunneling rate, and T_1^{-1} is obtained from the saturation in $I_{\uparrow\uparrow} - I_{\uparrow\downarrow}$ with bias voltage.

Finally, we must deduce the relative magnitude of T_1^{-1} . The rate of spin-flip transitions is expected to be significantly smaller than τ_{e-ph}^{-1} .¹⁸ In this case, the ground state would not necessarily be accessible by energy relaxation. The grain

could remain in an excited, spin-polarized state, as sketched in Fig. 4(C). These spin-polarized excited states are responsible for spin accumulation in the antiparallel magnetic configuration of the leads. If the relaxation rates for the spin-flip transitions are much smaller than the tunneling rate, then various spin-polarized states would have similar probabilities, which are determined by the tunneling rates. In the antiparallel configuration of the leads, the probabilities of the excitations with spin up would be enhanced by $1+P$, and probabilities of the excitations with spin down would be suppressed by $1-P$, where P is the spin polarization in the leads. In the parallel configurations, the probabilities of the excitations with spin up and spin down are the same. In this regime, $I_{\uparrow\uparrow} - I_{\uparrow\downarrow}$ is proportional to the current, similar to the usual ferromagnetic tunneling junctions.

It is reasonable to expect that the spin-flip rate $T_1^{-1}(\omega)$ increases rapidly with energy difference ω between the initial and the final states.²⁴ If $T_1^{-1}(\omega)$ exceeds the tunneling rate above some ω , then the excitations with energy $> \omega$ will occur with a reduced probability, in the ensemble of states generated by tunneling in and out. Thus, ΔI is limited by tunneling via the ground state and those low-lying spin-polarized states, where $T_1^{-1}(\omega) < \Gamma_L$. Here, ΔI versus bias voltage approaches saturation approximately when $T_1^{-1}(\omega) = \Gamma_L$, where ω is the highest excitation energy in the

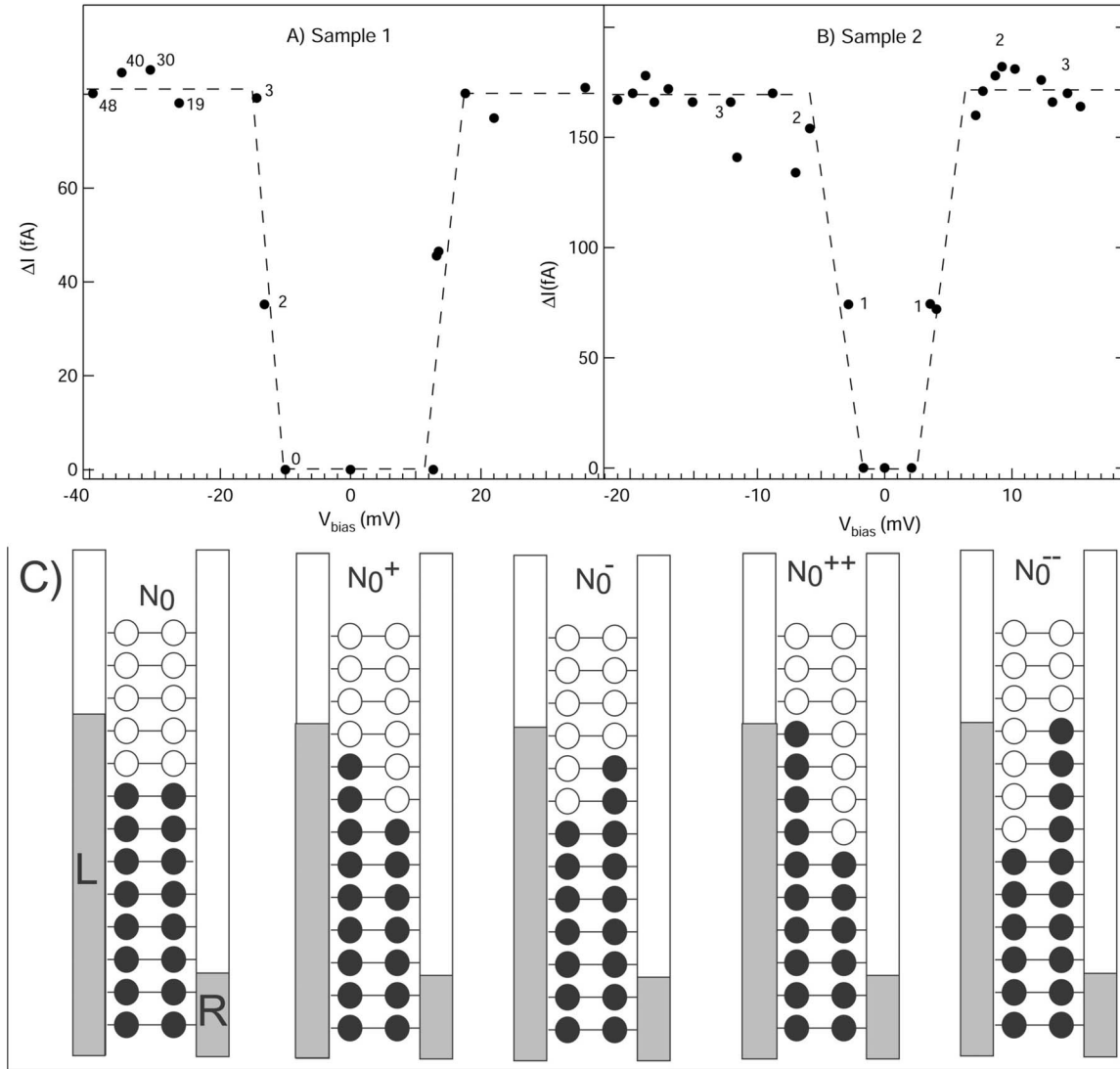


FIG. 4. (A) and (B): $\Delta I = |I_{\uparrow\uparrow} - I_{\downarrow\downarrow}|$ versus bias voltage in samples 1 and 2, respectively, at the base temperature. The numbers near the circles indicate how many doubly degenerate electron-in-a-box levels are available for tunneling in. (C): possible spin-polarized electron configurations caused by electron tunneling in and out, before an electron tunnels in, at the second current plateau, for N_0 even.

ensemble of spin-polarized states generated by tunneling in and out: $\omega \approx \delta_{|e|\Gamma_L}$. This is how we determine the spin-relaxation time $T_1^{-1}(\omega)$ at an energy ω in a given sample.

In sample 1, ΔI is at 50% of the saturation value at the second current plateau, and ΔI is saturated at the third current plateau. At the second current plateau, the spin-relaxation rate of the highest energy excited state generated by tunneling must be close to the tunneling rate. Since the spin relaxation is very rapid in configurations more than 3δ above the ground state, and N_0 is even as noted above, the grain spends most of the time among the five configurations shown in Fig. 4(C): N_0 , N_0^+ , N_0^- , N_0^{++} , and N_0^{--} . The highest energy spin-polarized states are N_0^{++} and N_0^{--} . Thus, $T_1^{-1}(3\delta) \approx \Gamma_L = 1.5 \times 10^6 \text{ s}^{-1}$. In sample 2, this analysis leads to $T_1^{-1}(2\delta) \approx 10^7 \text{ s}^{-1}$.

Now we discuss the origin of spin relaxation and its rapid enhancement with the energy difference. Note that the rate of spin-conserving transitions in Eq. (1) increases as ω .³ We suggest that the electron-phonon transition rates without and

with spin-flip scale by the Elliot-Yafet relation: $T_1^{-1}(\omega) = \alpha' \tau_{e-ph}^{-1}(\omega)$. This scaling would certainly explain the rapid increase in spin-relaxation rate with excitation energy. In metallic films, it is well established that the Elliot-Yafet scaling applies for both elastic and inelastic scattering processes, with $\alpha \approx \alpha'$.¹⁹

In sample 1, Eq. (1) leads to $\tau_{e-ph}^{-1}(3\delta) \approx 4 \times 10^{10} \text{ s}^{-1}$. Since $T_1^{-1}(3\delta) \approx 1.5 \times 10^6 \text{ s}^{-1}$, we obtain $\alpha' \approx 0.4 \times 10^{-4}$. Similarly, in sample 2, $\tau_{e-ph}^{-1}(2\delta) \approx 3.3 \times 10^{11} \text{ s}^{-1}$, and we obtain $\alpha' \approx 0.3 \times 10^{-4}$. Here, α' agrees with $\alpha \approx 1.5 \times 10^{-4}$ obtained earlier, within an order of magnitude. So the ratio of τ_{e-ph} and T_1 is in agreement with the Elliot-Yafet scaling. This is an evidence that the spin-flip transitions in Al grains are driven by the spin-orbit interaction. By this relaxation mechanism, the spin of an electron on the grain is coupled to the phonon continuum via the spin-orbit interaction. An electron in an excited spin-polarized state relaxes by an emission of a phonon, which has an angular momentum equal to the difference between the initial and final electron spins.

VI. CONCLUSION

In summary, we have observed spin-coherent sequential electron tunneling via discrete energy levels of single Al grains. Spin-polarized current saturates quickly as a function of bias voltage, which demonstrates that only the ground state and the few lowest excited states can carry spin-polarized current in these samples. Higher excited states have a relaxation time shorter than the tunneling time, and they do not carry spin-polarized current. The spin-relaxation times of the low-lying excited states are $T_1 \approx 0.7$ and $0.1 \mu\text{s}$ in two samples. Finally, the ratio of the electron spin-flip transition rate and the electron-phonon relaxation rate is in

quantitative agreement with the Elliot-Yafet scaling ratio, an evidence that the spin-relaxation transitions are driven by the spin-orbit interaction and phonons.

ACKNOWLEDGMENTS

This work was performed in part at the Georgia-Tech electron microscopy facility. We thank Matthias Braun and Markus Kindermann for consultation. This research is supported by the DOE under Grant No. DE-FG02-06ER46281 and David and Lucile Packard Foundation under Grant No. 2000-13874.

-
- ¹D. C. Ralph, C. T. Black, and M. Tinkham, *Phys. Rev. Lett.* **74**, 3241 (1995).
- ²O. Agam, N. S. Wingreen, B. L. Altshuler, D. C. Ralph, and M. Tinkham, *Phys. Rev. Lett.* **78**, 1956 (1997).
- ³D. Davidović and M. Tinkham, *Phys. Rev. Lett.* **83**, 1644 (1999).
- ⁴J. R. Petta and D. C. Ralph, *Phys. Rev. Lett.* **87**, 266801 (2001).
- ⁵C. T. Black, D. C. Ralph, and M. Tinkham, *Phys. Rev. Lett.* **76**, 688 (1996).
- ⁶M. Johnson and R. H. Silsbee, *Phys. Rev. Lett.* **55**, 1790 (1985).
- ⁷F. J. Jedema, H. B. Heersche, A. T. Filip, J. J. A. Baselmans, and B. J. van Wees, *Nature (London)* **416**, 713 (2002).
- ⁸M. Braun, J. König, and J. Martinek, *Europhys. Lett.* **72**, 294 (2005).
- ⁹I. Weymann and J. Barnas, *Phys. Rev. B* **73**, 205309 (2006).
- ¹⁰S. J. van der Molen, N. Tombros, and B. J. van Wees, *Phys. Rev. B* **73**, 220406(R) (2006).
- ¹¹W. Wetzels, G. E. W. Bauer, and M. Grifoni, *Phys. Rev. B* **74**, 224406 (2006).
- ¹²A. Cottet and M. S. Choi, *Phys. Rev. B* **74**, 235316 (2006).
- ¹³A. Cottet, T. Kontos, S. Sahoo, H. T. Man, M. S. Choi, W. Belzig, C. Bruder, A. F. Morpurgo, and C. Schonenberger, *Semicond. Sci. Technol.* **21**, S78 (2006).
- ¹⁴L. Zhang, C. Wang, Y. Wei, X. Liu, and D. Davidović, *Phys. Rev. B* **72**, 155445 (2005).
- ¹⁵F. Ernult, K. Yakushiji, S. Mitani, and K. Takanashi, *J. Phys.: Condens. Matter* **19**, 1652140 (2007).
- ¹⁶A. Bernand-Mantel, P. Seneor, N. Lidgi, M. Munoz, V. Cros, S. Fusil, K. Bouzouane, C. Deranlot, A. Vaures, F. Petroff *et al.*, *Appl. Phys. Lett.* **89**, 062502 (2006).
- ¹⁷S. Adam, M. L. Polianski, X. Waintal, and P. W. Brouwer, *Phys. Rev. B* **66**, 195412 (2002).
- ¹⁸Y. Yafet, *Solid State Phys.* **14**, 1 (1963).
- ¹⁹F. J. Jedema, M. S. Nijboer, A. T. Filip, and B. J. van Wees, *Phys. Rev. B* **67**, 085319 (2003).
- ²⁰G. Bergman, *Phys. Rep.* **107**, 1 (1984).
- ²¹J. Barnas and A. Fert, *Phys. Rev. Lett.* **80**, 1058 (1998).
- ²²J. S. Moodera, J. Nowak, and R. J. M. van de Veerdonk, *Phys. Rev. Lett.* **80**, 2941 (1998).
- ²³S. Zhang, P. M. Levy, A. C. Marley, and S. S. P. Parkin, *Phys. Rev. Lett.* **79**, 3744 (1997).
- ²⁴In bulk metals, the spin-orbit scattering rate increases rapidly with electron excitation energy.